Australian Journal of Basic and Applied Sciences, 7(5): 108-115, 2013
ISSN 1991-8178

Preparation and Characterisation of PolyamideHomopolymer and Block Copolymer Nanocomposites

[1,2]Khairul Anwar A.H., [1]James E. Kennedy, [1]Joseph B. Farrell

[1]School of Engineering, Athlone Institute of Technology (AIT), Dublin Road, Athlone, Co. Westmeath, Ireland.
[2]School of Materials Engineering, Universiti Malaysia Perlis, Perlis, Malaysia.

Abstract: Polyamidehomopolymer and block copolymernanocomposites were prepared by melt processing using a co-rotating Leistritz twin screw extruder. The polymers used werepolyamide 11 (PA11) and poly (ether-*block*-amide), Pebax 7233. Commercially available nanoclay, Cloisite 30B was chosen as the nanofiller in this study. Particular emphasis was placed on better defining the morphological and performance characteristics of the nanocomposites prepared.Analytical techniques such as X-ray diffraction (XRD), differential scanning calorimetry (DSC), dynamic mechanical analysis (DMA), and short-term mechanical tests were employed to characterise the nanocomposite materials.XRD analysis confirmed an exfoliated structure for PA11 nanocomposite at low loading whereas for Pebax 7233, an increase in d_{001} spacing suggests an intercalated structure exists. There was no significant change in melting temperature for PA11 and Pebax 7233 due to nanoclay addition; however, the crystallinity was found to decrease as measured by DSC.The performance characteristics of both nanocomposites systems were established using short-term tensile and DMA techniques.A significant increase in storage modulus was observed for both nanocomposite systems investigated.

Key words: Polyamide 11, Poly (ether-*block*-amide), nanoclay, polymer nanocomposites, X-ray diffraction, DSC, DMA, tensile stress-strain.

INTRODUCTION

Polyamide 11 is analiphatic partly crystalline homopolymerand has been commercially available since the mid-1950s(Sibila *et al*., 1995, Apgar, 1995, Xenopoulus and S. Clark, 1995).It is derived from the polymerisation of 11-amino undecanoic acid and is characterised by high tensile strength and stiffness, low water absorption and high ductility. The physical and mechanical properties of PA11 are principally affected by the presence of the highly polar amide(–CONH–) groups and the length of the hydrocarbon backbone.The presence of the former allows for hydrogen bonding between chains. It is the presence of these hydrogen bonds between adjacent polymer molecules that determine the melting point of the polymer. There is potential also for hydrogen bonds to form between the polymer chains and smaller polar molecules.

In the early 1970s, various research groups explored the possibility of synthesizing polyamide copolymers by covalently linking low molecular polyamide segments to soft polyether segments via amide, urethane or urea linkages. This typically resulted in in the formation of non-isomorphous polyamide copolymers,with the degree of crystallinity of the copolymer being significantly lower than that of the respective homopolymers.It was not until the discovery of the tetraalkoxide catalyst family by Atochem in later years that synthesis of high molecular weight polyamide block copolymers was made possible.

The polyamide copolymer materials of particular interest in study comprise linear chains of hard polyamide (PA) blocks covalently linked to soft polyether (PE) blocks via ester groups. These copolymers are referred to as segmented block copolymers, meaning that they have a soft segment that provides flexibility and a hard segment that provides strength. The hard segment is capable of forming rigid, hydrogen bonded crystalline phases with a high melting temperature, typically greater than 170 ^{o}C. The soft segment is generally derived from an amorphous polymer and has a low glass transition temperature, of the order of –40 ^{o}C.

Polymer - layered silicate nanocomposites, first reported in 1961, are attracting significant attention worldwide from both academic and industrial perspectives (Okamoto, 2003, Alexandre and Dubois, 2000). The two major findings that have triggered the revival of interest in this area were firstly; a report by Kojima and co-workers (Kojima *et al*., 1993) on Nylon-6/montmorillonite (MMT) nanocomposite, for which very small amounts of layered silicate loadings resulted in pronounced improvements of thermal and mechanical properties; and secondly, by Vaia*et al.*(Vaia *et al*., 1993) from their observation that it is possible to melt-mix polymers with layered silicates, without the use of organic solvents. In recent years, extensive efforts in developing polymer layered silicate nanocomposite are being conducted using almost all types of polymer matrices.

Corresponding Author: Khairul Anwar A.H., [1]School of Engineering, Athlone Institute of Technology (AIT), Dublin Road, Athlone, Co. Westmeath, Ireland.
E-mail: akhairul@research.ait.ie

In general, montmorillonite clay is hydrophilic and not compatible with most organic molecules. In order to make the hydrophilic phyllosilicates more organophilic, the hydrated cations of the interlayer can be exchanged with cationic surfactants alkylammonium or alkylphosphonium (onium) (Alexandre and Dubois, 2000, Pavlidou and Papaspyrides, 2008). According to Ray *et. al*(Sinha Ray and Okamoto, 2003), the role of alkylammonium or alkylphosphoniumcations in the organosilicates is to lower the surface energy of the layered silicate in order to reduce the electrostatic interactions between the layers, improve the wetting characteristic with polymer and allow molecules to diffuse between the layers. Additionally, the alkylammoniumcations provide functional groups that can react with the polymer or initiate polymerisation of monomers to improve the strength of the interface between the inorganic and the polymer. The replacement of inorganic exchange cations by organic onium ions on the gallery surfaces of smectite clays not only serves to match the clay surface polarity with the polarity of the polymer, but it also expands the clay galleries (Pavlidou and Papaspyrides, 2008, Sinha Ray and Okamoto, 2003). This facilitates the penetration of the gallery space intercalation by either the polymer precursor or preformed polymer.

This paper provides a thorough investigation on the effect of the nanoclay addition on the structure-property behaviour of polyamide homopolymer and block copolymer nanocomposites. This includes an examination of the morphological structures in both polymer matrices using XRD. Differences in thermal,thermo-mechanical and short-term mechanical properties of the nanocomposites compared to the virgin matrices will be discussed in terms of microstructure and polymer clay interaction. The performance comparison due to nanoclay addition within both polymer matrices will be also reported.

Experimental:

Materials:

The polyamide materials used in this work were PA11, trade name Rilsan B, Besvoa, and poly (ether-*block*-amide) under trade name Pebax (Pebax 7233) obtained from Arkema, France. The organically modified layered silicate used in this study was Cloisite 30B, a natural montmorillonite modified with a quaternary ammonium salt obtained from Southern Clay Products Co. USA.

Preparation Of Polyamide Based Nanocomposites:

PA11, Pebax 7233 granules and Cloisite 30B nanoclay powder were dried in a Piovan DSN 504 desiccant drier at 80^{o}C for 8 hours and at 75^{o}C for 24 hours respectively. The nanocomposites were prepared by melt blending and the compounding process was carried out on a Leistritz Micro 27 twin screw extruder with a 27mm screw diameter and a 38/1 length to diameter (L/D) ratio. The die temperature was maintained at 195^{o}C for Pebax 7233 and at 230^{o}C for PA11 with a screw speed of 120 rpm was used for both materials respectively. Nanocomposites with 2 wt% and 6 wt% nanoclay loading were prepared for both polymer matrix investigated.The nanocomposites were injection moulded to prepare samples of dimensions suitable for mechanical testing. A 350 kNArburg injection moulding machine was used to carry out the work. An ASTM D638 Type IV mould standard was used to prepare the tensile samples.

Characterisation Of Nanocomposite Morphology:

Crystal structure of the nanoclay powder and nanocomposite specimens were characterised by means of X-ray diffraction (XRD), using Bruker AXS X-ray diffractometer, equipped with Cu Kα1 radiation, λ = 1.5406 Å. The XRD was operated at 40kV and 30mA, at a scanning rate of 2^{o}/min, between 0^{o} to 40^{o} of 2θ angle. The interaction of elemental component due to nanoclay incorporated within polymer matrix was studied using this technique.

Thermal Analysis:

The effect of incorporating nanoclay on the melting behaviour of PA11 and Pebax 7233 was investigated using DSC. Virgin matrix and nanocomposites samples were studied using a Perkin Elmer Pyris 6 DSC unit in accordance to ASTM D3417. Samples weighing approximately 10 mg were used for analysis. A first scan was carried out to eliminate previous thermal history and the results of the second scan in the range of 25 ^{o}C to 250 ^{o}C at a heating rate of 10 ^{o}C/min were recorded. The instrument was calibrated using indium as a standard. Dynamic mechanical analysis (DMA) studies were carried out using a TA DMQ-800 instrument in accordance with ASTM D6110. The test was carried out in single cantilever mode, using a sample of dimension 17 mm x 12 mm x 2mm, over a wide temperature range from -130 ^{o}C to 150 ^{o}C. 1 Hz test frequency was used and a heating rate of 3 ^{o}C/min was maintained.

Mechanical Testing:

Tensile testing of PA11/ Cloisite 30B and Pebax 7233/Cloisite 30B nanocomposites was performed on an Instron 3365 universal testing machine using a 5 kN load cell with a crosshead speed of10 mm/min. Injection moulded Type IV dumbbell shape specimen was used and in all cases. The test was carried out in accordance

with ASTM 638 at ambient temperature. A minimum of 5 test specimens were tested from each batch where the average data will be presented later in this paper.

RESULTS AND DISCUSSION

XRD patterns of the pristine Cloisite 30B nanoclay, PA11/Cloisite 30B and Pebax 7233/Cloisite nanocomposites are presented in Figure 1. From these patterns, the (001) basal reflections are tabulated in Table 1 where the (001) diffraction peak of Cloisite 30B nanoclay is registered at $2\theta = 4.72^{o}$ with interlayer spacing (d_{001}) of 18.71 Å. These values are in agreement with those reported by other researchers (Yang and Tsai, 2007, Mohamadi and S. Sanjani, 2009, Ramadan *et al*., 2010, Yang and Tsai, 2006). In addition to the values obtained, the crystallite size of Cloisite 30B was calculated using Scherrer equation (Jenkins and L. Snyder, 1996)and the value obtained was 12 nm.

Polyamide 11 with 2 wt% nanoclay loading exhibited smooth scattering profiles, and absence of any basal reflections, which is indicative of disruption of the ordered silicate layers structure.The absence of the basal reflections peak indicates the delamination and dispersion of the silicate layers within the PA11 matrix, suggesting the formation of an exfoliated nanostructure. These results are in agreement with the previously reported work by Paul and Robeson (Paul and Robeson, 2008) and Zhang *et. al* (Zhang *et al*., 2004, Liu *et al*., 2003). Furthermore, in spite of the absence of the basal plane, a broad shoulder at a low 2θ angle region was observed for nanocomposite containing high clay concentration (6 wt%), which probably indicates a mixture of partially exfoliated and partially intercalated nanostructures.

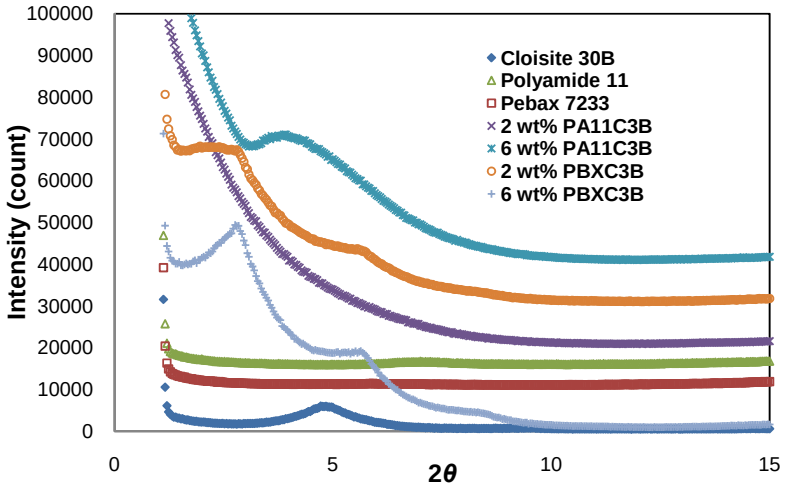

Fig. 1: XRD spectra of Cloisite 30B, PA11/Cloisite 30B and Pebax 7233/Cloisite 30B nanocomposites

In investigating Pebax nanocomposites, the initial 2θ angle shifted from 4.72^{o} to 2.84^{o} (Bragg's angle) whereas, the d_{001} spacing was found to increase from 18.71 Å to 31.08 Å. This increase indicates that interlayer structure of the nanoclay particles swelled due to intercalation of Pebax chains between the nanoclay platelets which is in agreement with the findings by I-Kuan*et. al* and Mohamadi *et. al*(Yang and Tsai, 2007, Mohamadi and S. Sanjani, 2009). Similar observations were also reported by Lim *et. al*(Lim and Park, 2001) when a shift in 2θ angle to a lower degree suggested that a partially intercalated structurewas formed when investigating poly(styrene-butadiene-styrene)/clay nanocomposites.

Table 1: XRD characteristics of Cloisite 30B, PA11/Cloisite 30B and Pebax 7233/Cloisite 30B nanocomposites

Material	2θ (^{o})	Interlayer spacing, d_{001} (Å)
Cloisite 30B	4.72	18.71
Polyamide 11	*Not observed*	-
2 wt% PA11C3B	*Not observed*	-
6 wt% PA11C3B	4.00	17.56
Pebax 7233	*Not observed*	-
2 wt% PBXC3B	2.84	31.08
6 wt% PBXC3B	2.84	31.08

In general, the exfoliation of clay platelets in a polymer matrix is the desired goal for formation of nanocomposite structures. The main factor that influences the polymer-clay interaction is the affinity the polymer matrix has for the silicate surface. Regarding the nanoclay used in this study, it was modified with ammonium salts comprising single alkyl (tallow) tail. This surfactant has a hydroxyl group attached to either the tallow tail or the ammonium head. The organic surfactant has the ability to increase the intergallery distance while maintaining sufficient organoclay interlayer spacing which is needed to overcome the cohesive forces between neighbouring platelets, thus facilitating polymer intercalation during melt blending. Considering the polymer materials used in this work are relatively polar and thus are capable of facilitating high degrees of hydrogen bonding, the difference in formation of nanocomposite structures in both systems as observed from the XRD spectra is believed to be influenced by the affinity that the polyamide structure has for the polar surface of the organoclay.

Thermograms of PA11 and Pebax 7233 presented in Figure 2 show endothermic peaks at 190 ^{o}C and 172 ^{o}C respectively, which correspond to the crystalline melting temperature of this partly crystalline matrix. It can be seen that the addition of Cloisite 30B nanoclay appears to have no significant effect on the melting temperature of both PA11 and Pebax 7233; however, the enthalpies of melting (ΔH) decreased as presented in Table 2. In the case of PA11, a minor endothermic peak was also observed at 183 $^{\circ}$C which is believed to be due to melting of small crystals in the inter-lamellar layers between the larger crystallites from secondary crystallisation (recrystallisation during heating). Polyamide 11 has high crystallisation rate and shows two melting peaks which corresponds two forms of crystal, or one type of crystal exhibiting different sizes or degrees of perfection (Zhang *et al*., 2004). In addition, under different conditions of crystallisation and temperature, one crystal form may transform into the other, and may show only one endothermic peak in the DSC thermogram. Similar observations were also reported by Zhang (Zhang *et al*., 2004) and Weng(Weng *et al*., 2003) in their work on crystallisation studies of PA11 nanocomposites and polyamide 6 nanocomposites respectively. The existence of the small endothermic peak as observed for virgin PA11 was not evident in the nanocomposite systems.

The degree of crystallinity (X_c) of the PA11, Pebax 7233 and their nanocomposites was calculated using Eq. 1 and the values obtained are presented in Table 2.

$$X_c = (\Delta H_f / \Delta H_f^*) \times 100 \quad (1)$$

where ΔH_f is the enthalpy of fusion recorded from the thermograms and ΔH_f^* is the enthalpy of fusion of perfect crystalline polymer; ΔH_f^* quoted for PA11 and PA12 (*composition of 80 mol % PA 12 phase in Pebax 7233)*are 162.5 J/g (Apgar, 1995, Mark, 1999) and 246 J/g(Armstrong *et al*., 2012)respectively.

With reference to Table 2, it is believed that the decrease in crystallinity as observed in PA11 and Pebax 7233 can probably be attributed to the change in the morphology of the matrix phase due to nanoclay dispersion. The presence of high concentrations of dispersed nanoclay platelets prevents large crystalline domains from forming due to limited space and restrictions imposed on polymer chains by a high number of silicate platelets; this leads to smaller crystallite structures and more imperfectly formed crystalline lamella (Yu *et al*., 2009, Fornes and Paul, 2003). A number of researchers working on polymer nanocomposite systems also reported a reduction in percentcrystallinity due to nanoclay addition (McNally *et al*., 2003, Fornes and Paul, 2003, Shen *et al*., 2004, Gopakumar *et al*., 2002).

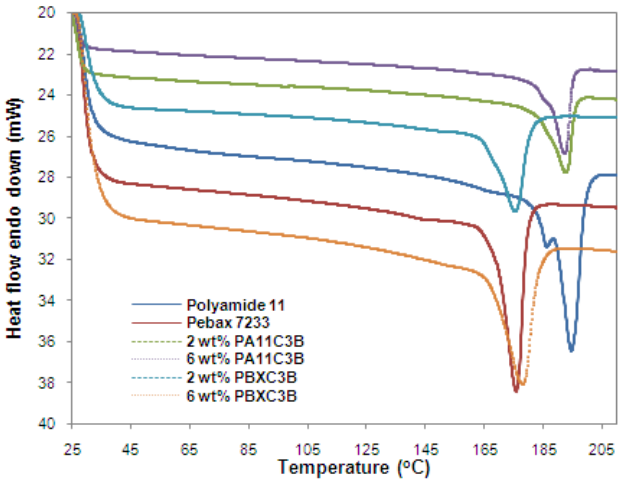

Fig. 2: Enthalpy as a function of temperature for PA11/Cloisite 30B and Pebax7233/Cloisite 30B nanocomposites

Table 2: Thermal properties of PA11/Cloisite 30B and Pebax 7233/Cloisite 30B nanocomposites

Materials	Melting Point T_m (°C)	Enthalpy of Fusion, ΔH (J/g)	Crystallinity, X_c (%)
Polyamide 11	190.53	60.37	37.15
2 wt% PA11C3B	191.60	54.87	33.77
6 wt% PA11C3B	190.60	51.03	31.40
Pebax 7233	172.51	55.63	18.09
2 wt% PBXC3B	172.35	43.92	14.28
6 wt% PBXC3B	172.06	44.83	14.57

Temperature dependence of loss tangent and dynamic storage modulus for PA11 and Pebax 7233 are presented in Figure 3. Polyamide 11 and Pebax 7233 exhibited three main relaxation peaks, defined at decreasing temperatures as α, β and γ as tabulated in Table 3 where the β and γ relaxations are the sub-T_g transitions and associated with the material properties in the glassy state. In this case, the γ relaxation corresponds to the local motion of methylene sequences that exist in both amorphous polyamide phases. As the test temperature rises, the free volume increases so that localised bond and side chain movements can occur. It was found that the β relaxation for PA11 occurred approximately at -70 °Ccan be assigned to localised movement of chain segments, including the amide groups which are not involved in hydrogen bonding (McGrum *et al*., 1991). For Pebax 7233, the β relaxation approximately at -74 °Cindicates the point where polyether phase undergoes a softening which arises from the glass transition behaviour of the polyether segment (Sheth *et al*., 2003).

The glass transition T_g represents a major transition for many polymers, as physical properties changes considerably as the material goes from a hard glassy state to a soft rubbery state. At still higher temperatures the α relaxation for PA11 observed at 52 °C, corresponds to the temperature at which mobility of the main-chain segments within amorphous regions of the polymer occurs; it is thus directly related to the glass transition temperature T_g. For Pebax 7233, the αrelaxation occurred at 28 °Cand corresponds to the glass transition of the PA12 hardsegment. These findings are in broad agreement with dynamic studies carried out by Sheth(Sheth *et al*., 2003, J.P and G.L., 2005).

With reference to Table 3, it can be seen that by dispersing nanoclay within both matrix resulted significant increase in storage modulus. Upon 2 wt% nanoclay addition, the storage modulus at room temperature (25°C) improved by up to 55% compared to the virgin matrix alone. Improvements in storage modulus for nanocomposites are as a result of strong interfacial interactions between the polymer and the clay platelets, reduced mobility of polymer chains confined between or bonded to the clay surfaces and the inherent highmodulus of the clays.

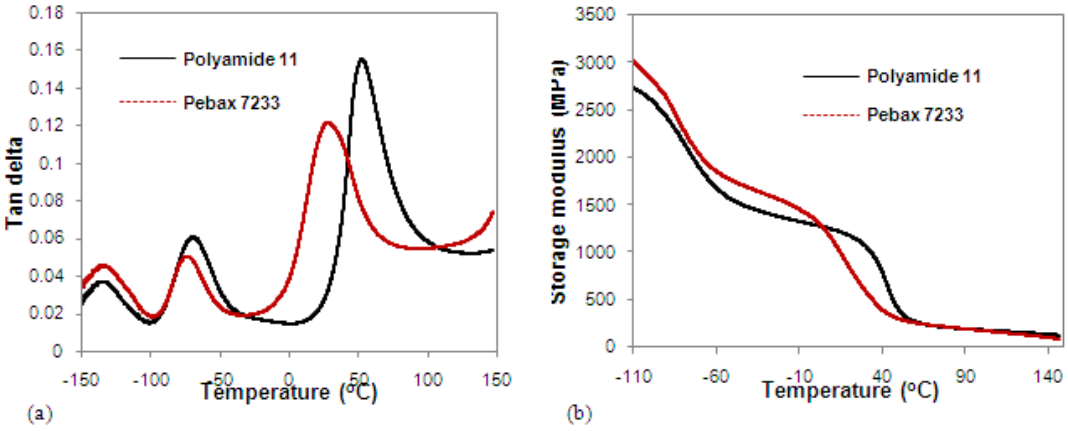

Fig. 3: (a) Loss tangent (tan δ) as a function of temperature for PA11 and Pebax 7233
(b) Storage modulus as a function of temperature for PA11 and Pebax 7233

Table 3: DMA data for PA11/ Cloisite 30B and Pebax 7233/Cloisite 30B nanocomposites

Material	Relaxation			Storage modulus at 25°C (MPa)
	γ (°C)	β (°C)	α (°C)	
Polyamide 11	-150	-70.17	51.20	1133.00
2 wt% PA11C3B	-	-73.06	52.14	1845.00
6 wt% PA11C3B	-	-72.84	48.27	2044.00
Pebax 7233	-150	-73.97	27.39	711.10
2 wt% PBXC3B	-	-72.65	28.41	1103.00
6 wt% PBXC3B	-	-77.02	28.17	1243.00

Figure 4 illustrates stress-strain responsestypical of those recorded for PA11, Pebax 7233 and PA11 and Pebax nanocomposites.Selected tensile stress-strain data are also presented in Table 4. An increase in the ultimate tensile strength of 15.12 % and an increase in strain at break of 12.33 % was observed for 2 wt% PA11C3B. The incorporation of 6 wt% nanoclay resulted in an increase of ultimate tensile strength of 22.61 % and strain at break of 14.70 %. In the case of Pebax 7233, addition of 2 wt% of Cloisite 30B nanoclay resulted an increase in ultimate tensile strength of 24.22 % and the strain at break increased by 4.25 %. At 6 wt% nanoclay loading, an ultimate tensile strength of 73.12 MPa and strain at break value of 389.56 % were recorded. The tensile modulus values for both nanocomposites systems show complementary behaviour to the DMA storage modulus data presented earlier; a significant increase in tensile modulus, up to 52.37 % for the PA11 and 118.64 % forPebax 7233 was recorded.

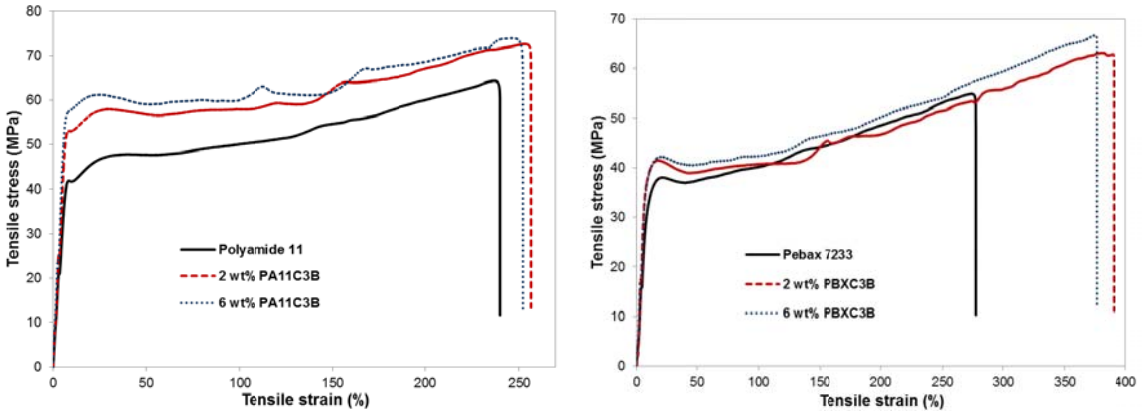

(a) (b)

Fig. 4: Typical stress-strain response for (a) PA11/Cloisite 30B nanocomposites (b) Pebax/Cloisite 30B nanocomposites

It is noteworthy that while the tensile strain at break of conventional polymer-inorganic filled composites is low, typically no more that a few percent, the strain at break values recorded for the PA11 and Pebax 7233 nanocomposite systems prepared in this study are greater than those recorded for the virgin matrices. This would suggest that the matrix morphology has been modified somehow, probably in the same way as outlined by Li (Li *et al*., 2007). They observed that the effect of the clay platelets was to reduce PA6 crystal size dramatically. The small but significant increase in strain at break observed further supports the evidence presented earlier that the well dispersed nanoclay platelets are effective in promoting heterogeneous nucleation but probably also hinder spherulite growth. Interestingly also, at comparable loadings of Cloisite 30B, the Pebax 7233 nanocomposites exhibit comparable ultimate tensile strength values to the PA11 materials.

Table 4: Tensile data for PA11/Cloisite 30B and Pebax/ Cloisite 30B nanocomposites

Material	Tensile Modulus (MPa)	Tensile stress (MPa)	Tensile strain (%)
Polyamide 11	800.24+/-15.33	60.63+/-3.10	221.70+/-20.38
2 wt% PA11C3B	1072.92+/-65.41	69.80+/-2.44	249.04+/-11.22
6 wt% PA11C3B	1219.74+/-62.41	74.34+/-1.51	254.29+/-7.39
Pebax 7233	514.09+/-11.37	57.12+/-0.89	318.48+/-4.68
2 wt% PBXC3B	895.96+/-53.69	68.02+/-1.76	336.46+/-18.88
6 wt% PBXC3B	1124.35+/-66.13	73.12+/-2.92	389.56+/-10.47

The primary aim of melt blending nanoclay into a homopolymer and block copolymermatrixis to improve the mechanical and thermal properties of the polymeric material. Nevertheless, such improvements can be only achieved when fillers constrain matrix deformation depending on the magnitude of which is a function of size, concentration, surface treatment, state of dispersion of the fillers and of the individual elastic properties of the fillers and matrix.The improvements in short-term mechanical properties of a thermoplastic polymer have been also reported by number of researchers working on polymer-clay nanocomposite systems (Sinha Ray and Okamoto, 2003, Alexandre and Dubois, 2000, Yasue *et al*., 2000, Aït Hocine *et al*., 2008, Wilkinson *et al*., 2007). Several explanations can be suggested regarding the reinforcing effect observed in clay filled polymers, based on interfacial properties and restricted mobility of the polymer chains. The reinforcing effect depends on three properties of the reinforcing material, namely rigidity, aspect ratio and the affinity with the polymer matrix (Yasue *et al*., 2000). In addition, the degree of exfoliation and dispersion of clay platelets in the polymer matrix also contributes to the reinforcing mechanism (Manias *et al*., 2001, Tjong, 2006).

Conclusions:

Polyamide homopolymer and block copolymer nanocomposites were melt blended using a twin screw extruder. The combination of XRD data revealed an exfoliated clay morphology within the PA11 matrix at a low clay loading but an intercalated clay morphology at higher clay loadings. In the case of Pebax 7233, the gain in d_{001}spacings suggests an intercalated clay morphology existed.It was confirmed by DSC that there was no significant changes in the melting temperature of either the PA11 or Pebax 7233 matrix. Addition of 2 wt% nanoclay within PA11 resulted 11 % decrease in crystallinity wherease for Pebax 7233, a 21 % decrease in crystallinity was observed. The decrease in crystallinity was probably a result of restricted movement of polymer chains due to strong dipole interaction between clay platelets and the polymer matrices. DMA results showed that a significant increase in storage modulus was observed for all nanocomposites prepared. Storage modulus for the PA11 composite containing 2 wt% nanoclay resulted in increase in storage modulus of 62 % whereas for Pebax 7233, the storage modulus was found to increase by 55 %. Furthermore, short-term mechanical propertiesof PA11 and Pebax 7233 were significantly improved. An increase in the ultimate tensile strength by 15.12 % and strain at break by 12.33 % were observed for PA11 melt blended with 2 wt% nanoclay. Addition of 2 wt% of Cloisite 30B nanoclay into Pebax 7233 resulted in an increase in ultimate tensile strength of 24.22 %, where the strain at break increased by 4.25 %. The increase in strain at break values can probably attributed to the changes in morphology observed in both nanocomposites systems.

ACKNOWLEDGMENTS

This work was funded by Athlone Institute of Technology (AIT), Universiti Malaysia Perlis (UniMAP) and Ministry of Higher Education Malaysia. Special thanks to the staff of AIT,MRI and Creagh Medical Limited, Ballinasloe for their support throughout the work.

REFERENCES

AÏT HOCINE, N., P. MÉDÉRIC, & T. AUBRY, 2008. Mechanical properties of polyamide-12 layered silicate nanocomposites and their relations with structure. *Polymer Testing,* 27: 330-339.

ALEXANDRE, M. & P. DUBOIS, 2000. Polymer-layered silicate nanocomposites: preparation, properties and uses of a new class of materials. *Materials Science and Engineering: R: Reports,* 28: 1-63.

APGAR, G., 1995. PA 11. *In:* I. KOHAN, M. (ed.) *Nylon Plastics Handbook.* Passau: Carl Hanser Verlag.

ARMSTRONG, S., B. FREEMAN, A. HILTNER, & E. BAER, 2012. Gas permeability of melt-processed poly(ether block amide) copolymers and the effects of orientation. *Polymer,* 53: 1383-1392.

FORNES, T.D. & D.R. PAUL, 2003. Crystallization behavior of nylon 6 nanocomposites. *Polymer,* 44: 3945-3961.

GOPAKUMAR, T.G., J.A. LEE, M. KONTOPOULOU & J.S. PARENT, 2002. Influence of clay exfoliation on the physical properties of montmorillonite/polyethylene composites. *Polymer,* 43: 5483-5491.

S, J.P. & G.L., W. 2005. Semicrystalline Segmented Poly(Ether-b-amide) Copolymers: Overview of Solid-State Structure Property Relationships and Uniaxial Deformation Behavior. *In:* FAKIROV, S. (ed.) *Handbook of Condensation Thermoplastic Elastomers.* Germany: WILEY-VCH Verlag GmbH.

JENKINS, R. & L.R. SNYDER, 1996. Diffraction theory. *In:* JENKINS, R. & L. SNYDER, R. (eds.) *Introduction to X-Ray powder diffractometry.* Wiley.

KOJIMA, T., AU., MK., A.O., T.K. & O.K. 1993. Synthesis of Nylon-6-clay Hybrid by Montmorillonite Intercalated with epsilon-Caprolactam. Japan.

LI, T.-C., J. MA, M. WANG, W.C. TJIU, T. LIU, & W. HUANG, 2007. Effect of clay addition on the morphology and thermal behavior of polyamide 6. Journal of Applied Polymer Science, 103: 1191-1199.

LIM, Y.T. & O.O. PARK, 2001. Microstructue and rheological of block copolymer/clay nanocomposites. *Korean Journal Chemical Engineering,* 1: 21-25.

LIU, T., K. PING LIM, W. CHAUHARI TJIU, K.P. PRAMODA, & Z.-K. CHEN, 2003. Preparation and characterization of nylon 11/organoclay nanocomposites. *Polymer,* 44: 3529-3535.

MANIAS, E., A. TOUNY, L. WU, K. STRAWHECKER, B. LU, & T.C. CHUNG, 2001. Polypropylene/Montmorillonite Nanocomposites. Review of the Synthetic Routes and Materials Properties. *Chemistry of Materials,* 13: 3516-3523.

MARK, E.J., 1999. *Polymer Data Handbook,* New York, Oxford University Press.

MCGRUM, N.G., B.E. READ, & G. WILLIAMS, 1991. Polyamides and Polyurethanes. *Anelastic and Dielectric Effects in Polymeric Solids*. New York: John Wiley & Sons.

MCNALLY, T., W. RAYMOND MURPHY, C.Y. LEW, R.J. TURNER, & G.P. BRENNAN, 2003. Polyamide-12 layered silicate nanocomposites by melt blending. *Polymer,* 44: 2761-2772.

MOHAMADI, S. & S. SANJANI, 2009. Studies on PEBAX/organoclay nanocomposites by melt intercalation process : Effect of organoclay. *e-Polymers*.

OKAMOTO, M., 2003. *Polymer/Layered Silicate Nanocomposites,* Shrewsbury, Rapra Technology Limited.

PAUL, D.R. & L.M. ROBESON, 2008. Polymer nanotechnology: Nanocomposites. *Polymer,* 49: 3187-3204.

PAVLIDOU, S. & C.D. PAPASPYRIDES, 2008. A review on polymer-layered silicate nanocomposites. *Progress in Polymer Science,* 33: 1119-1198.

RAMADAN, A.R., A.M.K. ESAWI, & A.A. GAWAD, 2010. Effect of ball milling on the structure of Na+-montmorillonite and organo-montmorillonite (Cloisite 30B). *Applied Clay Science,* 47: 196-202.

SHEN, L., I.Y. PHANG, L. CHEN, T. LIU, & K. ZENG, 2004. Nanoindentation and morphological studies on nylon 66 nanocomposites. I. Effect of clay loading. *Polymer,* 45: 3341-3349.

SHETH, J.P., J. XU, & G.L. WILKES, 2003. Solid state structure-property behavior of semicrystalline poly(ether-block-amide) PEBAX® thermoplastic elastomers. *Polymer,* 44: 743-756.

SIBILA, J.P., N.S. MURTHY, K.G. MINA, & E.M. MILTON, 1995. Characterization. *In:* MELVIN, I. K. (ed.) *Nylon Plastics Handbook.* Munich: Hanser Verlag.

SINHA, R.A.Y.S. & M. OKAMOTO, 2003. Polymer/layered silicate nanocomposites: a review from preparation to processing. *Progress in Polymer Science,* 28: 1539-1641.

TJONG, S.C., 2006. Structural and mechanical properties of polymer nanocomposites. *Materials Science and Engineering: R: Reports,* 53: 73-197.

VAIA, R.A., H. ISHII, & E.P. GIANNELIS, 1993. Synthesis and properties of two-dimensional nanostructures by direct intercalation of polymer melts in layered silicates. *Chemistry of Materials,* 5: 1694-1696.

WENG, W., G. CHEN, & D. WU, 2003. Crystallization kinetics and melting behaviors of nylon 6/foliated graphite nanocomposites. *Polymer,* 44: 8119-8132.

WILKINSON, A.N., Z. MAN, J.L. STANFORD, P. MATIKAINEN, M.L. CLEMENS, G.C. LEES, & C.M. LIAUW, 2007. Tensile properties of melt intercalated polyamide 6 - Montmorillonite nanocomposites. *Composites Science and Technology,* 67: 3360-3368.

XENOPOULUS, A. & S. CLARK, 1995. Physical Structure. *In:* I. KOHAN, M. (ed.) *Nylon plastics handbook.* Munchen: Carl Hanser Verlag.

YANG, I.-K. & P.-H. TSAI, 2007. Preparation and characterization of polyether-***block***-amide copolymer/clay nanocomposites. *Polymer Engineering & Science,* 47: 235-243.

YANG, I.K. & P.-H. TSAI, 2006. Intercalation and viscoelasticity of poly(ether-block-amide) copolymer/montmorillonite nanocomposites: Effect of surfactant. *Polymer,* 47: 5131-5140.

YASUE, K., S. KATAHIRA, & M., Y. 2000. *In Situ* Polymerization Route to Nylon 6-Clay Nanocomposites. *In:* T.J., P. & G.W., B. (eds.) *Polymer-Clay Nanocomposites.* West Sussex: John Wiley & Sons.

YU, W., Z. ZHAO, W. ZHENG, B. LONG, Q. JIANG, G. LI, & X. JI, 2009. Crystallization behavior of poly(vinylidene fluoride)/montmorillonite nanocomposite. *Polymer Engineering & Science,* 49: 491-498.

ZHANG, Q., M. YU, & Q. FU, 2004. Crystal morphology and crystallization kinetics of polyamide11/clay nanocomposites. *Polymer International,* 53: 1941-1949.